Urban Water Journal

ISSN: 1573-062X (Print) 1744-9006 (Online) Journal homepage: www.tandfonline.com/journals/nurw20

Comparison of urban overland flow dynamics on sealed and partially permeable surfaces across a European transect

Boney Anna Joseph, Nasrin Haacke & Eva Paton

To cite this article: Boney Anna Joseph, Nasrin Haacke & Eva Paton (2025) Comparison of urban overland flow dynamics on sealed and partially permeable surfaces across a European transect, Urban Water Journal, 22:5, 566-583, DOI: 10.1080/1573062X.2025.2495216

To link to this article: https://doi.org/10.1080/1573062X.2025.2495216

Published online: 23 Apr 2025.

URBAN WATER JOURNAL
2025, VOL. 22, NO. 5, 566–583
https://doi.org/10.1080/1573062X.2025.2495216

Taylor & Francis
Taylor & Francis Group

RESEARCH ARTICLE

OPEN ACCESS Check for updates

Comparison of urban overland flow dynamics on sealed and partially permeable surfaces across a European transect

Boney Anna Joseph [a], Nasrin Haacke [a,b] and Eva Paton [a]

[a]Ecohydrology, Institute of Ecology, TU Berlin, Berlin, Germany; [b]Research Group Groundwater, Kompetenzzentrum Wasser Berlin, Berlin, Germany

ABSTRACT

This study has analysed the extent to which overland flow dynamics, simulated with sub-hourly rainfall data for two scenarios of fully sealed and partially permeable urban streets, varies for 10 European cities across the Cfb climate zone. The cities showed similar behaviour in terms of frequency, total, peak flow and seasonality, with the exception of the western end of the Cfb transect. Introducing SUDS such as the partially permeable scenario reduced medium and large events in all cities; however; they were more pronounced in the central and north-eastern cities of transect. Long dry spells followed by large, flashier runoff events are prominent in some cities, increasing surface-water issues from diffuse pollution due to prolonged pollutant accumulation. The effects of temporal scaling of sub-hourly and hourly rainfall data on overland flow and the usability of ERA rain data were assessed to enable a coherent urban overland flow analysis relevant for pollution transport.

ARTICLE HISTORY
Received 27 May 2024
Accepted 7 April 2025

KEYWORDS
Overland flow; SUDS; diffuse pollution; sub-hourly rainfall

SUSTAINABLE DEVELOPMENT GOALS
SDG 6: Clean water and sanitation; SDG 11: Sustainable cities and communities

1. Introduction

Rapid urbanisation, along with climate change, has aggravated the issue of excess runoff and the resulting diffuse pollution from urban environments. The evaluation of the EU-commissioned Urban Wastewater Treatment Directive (UWWTD) in 2019 revealed the need to reduce stormwater runoff and combine sewer overflow spills (CSO) which was addressed in the new Directive proposal (European Commission 2022). Defining a better legal framework applicable to all European cities requires extensive technical information considering the different climatic and urban hydrological aspects across these cities. To set an EU-wide target for combined sewer overflow (CSO) spills, it is essential to gain a common understanding of the similarities and dissimilarities in the overland flow dynamics across European cities.

On European and global scales, previous studies on urban overland flow have mainly concentrated on rainfall extremes that generate significant overland flow, impacting public safety and causing economic losses. A majority of these previous studies aimed to quantify pluvial flood risk exposure in cities; for example, 20 European cities in Essenfelder et al. (2022), four specific European cities in Skougaard Kaspersen et al. (2017) and a review study for the entire UK by Miller and Hutchins (2017).

Moftakhari et al. (2018) pointed out that even though extensive research has been carried out on rainfall extremes and resulting flash flood events in cities, very little focus has been given to minor to medium overland flows. These events do not hamper public safety or cause economic loss, but they can disturb daily routines by disrupting traffic and adding stress to sewer systems. Therefore, steps towards sustainable storm water management must consider the entire scale, ranging from minor to extreme overland flow events. In addition to flooding, urban overland flow is responsible for transporting diffuse pollutants, resulting in major contribution to the ongoing detrimental ecological state of surface water, as per the EU Water Framework Directive (European Commission 2014). Rainstorms preceded by dry spells exacerbate pollution concentrations in overland flows (Soltaninia et al. 2023; Yang et al. 2021). When considering climate change and global warming, dry spells longer than 2 weeks are thought to have become more frequent in Western Europe (Breinl et al. 2020; Serra et al. 2016) making it more relevant to investigate the frequency of rainstorm events and the resulting overland flow events concurrent with these dry spells. Except for a few previous studies on rural catchments (Qiu et al. 2021; Santos et al. 2016), the concurrence of long dry spells (greater than 14 days) with large runoff events has been understudied.

The last decades saw a transition from conventional drainage systems, accompanied by heavily sealed areas in urban centres, towards sustainable drainage systems (SUDS) using a range of components for source control. Multiple studies demonstrated the runoff reduction potential of various measures such as rain gardens or partly permeable pavements in different urban set-ups (Abdalla et al. 2021; Arvand et al. 2023; Funke and Kleidorfer 2024). However, no inter-city comparison exists that evaluates and compares the reduction potential of SUDS for overland flow across a whole range of cities with their specific rainfall regimes.

With field data on urban overland flow mostly absent, the way forward to compare overland flow events across different urban settings, magnitude classes and SUDS components involve urban runoff modelling. Thus, classical urban drainage models can be used for basic signal processing to transform rainfall series into overland flow series by considering loss

CONTACT Boney Anna Joseph b.joseph@tu-berlin.de

factors due to infiltration, evaporation, interception and depression storage losses (Fletcher, Andrieu, and Hamel 2013). At the same time, urban drainage models are well equipped and validated to incorporate the effects of various SUDS measures (Ahmad et al. 2025; Funke and Kleidorfer 2024). The availability of a high-resolution rainfall series is crucial here, as concentration times are often short, making them highly sensitive to rainfall intensities (Aronica, Freni, and Oliveri 2005; Ochoa-Rodriguez et al. 2015).

For the majority of rain stations, although measurements occur at finer resolutions, data are available only at hourly or even daily intervals (Vorobevskii et al. 2024). Owing to the limited availability of high-resolution rainfall data, it is important to investigate the suitability of using more easily available hourly-resolution rainfall data to reproduce overland flow dynamics. Extensive studies (Berne et al. 2004; Bruni et al. 2015) on the effect of temporal scaling on hydrological responses have been restricted to a few selected extreme storm events. However, the effect of the temporal scaling of rainfall data from sub-hourly to hourly time resolutions in the modelling of overland flow dynamics is underinvestigated. For an EU-wide comparison aimed at supporting the formulation of framework directives, it is more feasible to utilise publicly available global long-term rainfall data derived from the ERA5 climate set (Copernicus Climate Change Service 2023), rather than using regional climate data from many different local sources. Previous studies (Kawohl 2019; Rivoire, Martius, and Naveau 2021) have compared ERA5 precipitation with observation data in terms of seasonal or annual mean daily precipitation, and they found reasonable agreement between the two datasets in Central Europe. However, climate models producing these data are known to underestimate the intensity of convective rainfall, known as drizzling bias (Chen, Dai, and Hall 2021; DeMott, Randall, and Khairoutdinov 2007). It is not clear how these shortcomings would be affected when ERA5-Land rain data is translated to overland flow. Therefore, the reliability of ERA5-Land data as a substitute for high-resolution station data in generating overland flow needs to be further investigated.

Despite many area-based and city-based studies, there is a gap in the common understanding of urban overland flow behaviour across Europe. For this purpose, we undertook an analysis of overland flow dynamics for 10 European cities across the northern coastal climate zone which enabled an inter-comparison of urban overland flow characteristics across an EU transect. This will, in turn, allow the interpretation of EU legislation based on a more common understanding of the similarities and differences in the overland flow dynamics in these regions. The initial hypothesis is that cities in the same climate zone would show similar overland flow behaviour for an urban street surface. Firstly, the study investigated how behaviour of overland flow events varies along the transect with respect to their total flow and peak characteristics, seasonality and concurrency of long dry spells followed by a large runoff event. Two scenarios were investigated in a typical urban context: a fully sealed street section and a street section incorporating SUDS components in the form of partially permeable pavements. Second, the effects of the temporal scaling of sub-hourly to hourly rainfall data on simulated overland flow events were quantified and compared across the EU transect. The final part of the analysis was to understand whether publicly available ERA5-Land hourly rainfall data can be used as a proxy for high-resolution data for overland flow analysis across the European transect.

2. Data and methodology

2.1. Study area and rainfall data

For the assessment of the overland flow dynamics, high-resolution rainfall series were collected for 10 cities across northern-central Europe, which is characterised by a temperate oceanic climate of the group Cfb (Koeppen-Geiger classification, Rubel et al. 2017, Figure 1). The Cfb group is the most dominant climate group in Europe with no significant rainfall differences between the seasons, the coldest month averaging above 0°C, at least one month's average temperature being above 22°C and at least four months averaging above 10°C (Rubel et al. 2017). The acquisition of long-term, high-resolution rainfall data is challenging. Whitford et al. (2023) discussed the difficulty in obtaining a series with a resolution of 1 to 6 h, let alone 1 min. Based on the availability of high-resolution rainfall data, 10 cities in Spain, France, Germany and Denmark were selected for the analysis (Figure 1, meta information in Table 1). To ensure a high-quality series with the smallest number of gaps, centennial observation stations (World Meteorological Organisation 2021) and airport stations were selected. Rainfall data with 1-min resolution are freely available for Germany (DWD Climate Data Center 2023) and Denmark (Danish Meteorological Institute- Open Data 2023). For Spain and France, 10 min (State Meteorological Agency AEMET 2023) and 6 min (Meteo France Public Data Portal 2023) rainfall data were available upon request from their respective meteorological offices. Recent sub-hourly rainfall series was not freely available for stations in the UK (1-min rainfall data were accessible only for the period 1986–2005) and there were no long-term, continuous station data from the Netherlands. The maximal shared temporal extent of the datasets covered the period 2012–2021, which was selected as the investigation period (although longer series were available for Germany, Spain and France).

Daily minimum and maximum temperature time series were obtained from the openly available European Climate Assessment & Dataset (Klein Tank et al. 2002).

The ERA5 hourly rainfall data were derived from the ERA5-Land dataset of the Copernicus Climate Change Service (2023), which is a replay of the land component of the fifth-generation ECMWF reanalysis ERA5 (ECMWF 2023). Gridded data for land surfaces were available at a spatial resolution of 9 × 9 km and a period of 1950–2023. The ERA5 hourly rainfall series for the 10 cities was derived from grid cells in the direct neighbourhoods of the rainfall stations (Table 1).

2.2. SWMM model, scenarios and their parameterisation

Overland flow dynamics for all stations across the transect was simulated for two street scenarios with the Storm Water Management Model (SWMM) (version 5.2, Rossman and Michelle 2022). The SWMM model is an open-source, dynamic drainage model that models water fluxes within urban

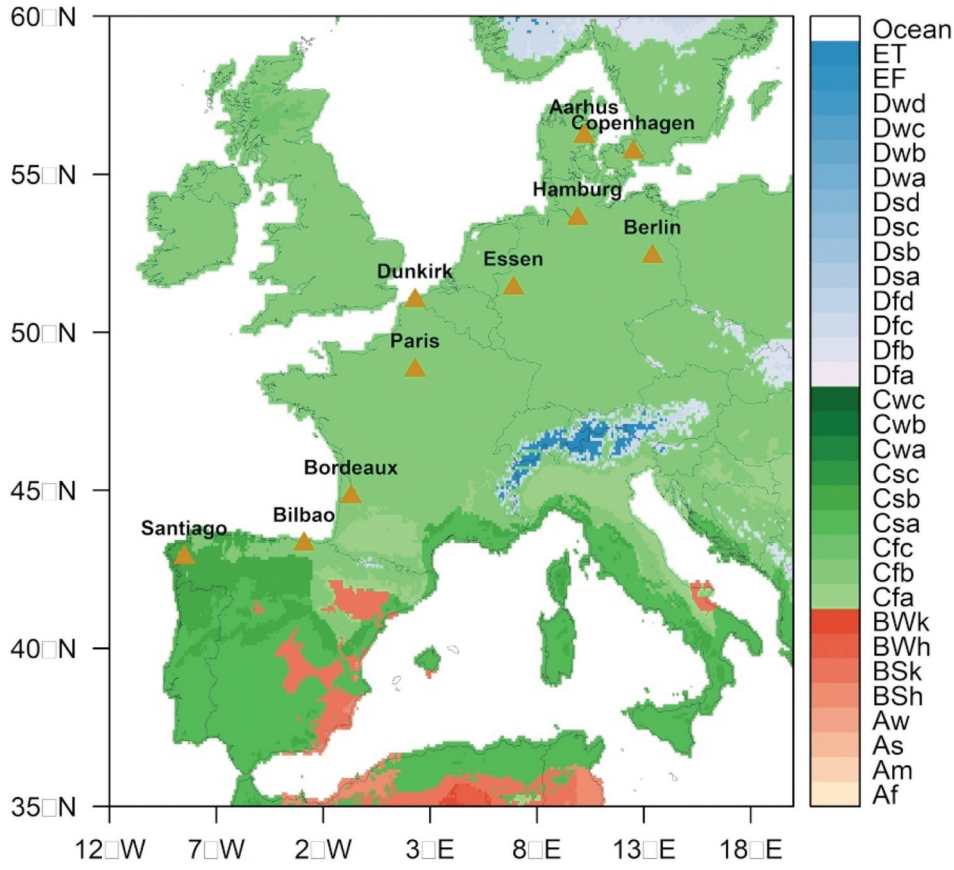

Figure 1. European transect across northern-central Europe within the temperate, oceanic climate of the group Cfb. Orange triangle: locations of the selected 10 cities and the climate zones after Koppen-Geiger (Rubel et al. 2017). Santiago de Compostela is partially influenced by another climate zone Csb.

Table 1. Metadata for the 10 cities across a European transect within the climate zone CfB including official station names and ids, latitude and longitude, and mean annual rainfall based on 2012–2021 data and temporal resolution.

Cities	Station name, ID (latitude, longitude)	Mean annual rain (mm)	Temporal resolution
Aarhus	Egå Renseanlæg, 5180 (56.2, 10.2)	650	1 min
Copenhagen	Københavns Lufthavn, 6180(55.61, 12.6)*	620	
Hamburg	Hamburg-Fuhlsbüttel, 1975 (53.6,9.9)	725	1 min
Berlin	Berlin-Tempelhof, 433 (52.4,13.4)	526	
Essen	Essen-Bredeney, 1303 (51.4, 6.9)	857	
Dunkirk	Dunkerque 59,183,001 (51.05, 2.33)**[1]	675	6 min
Paris	Paris- Montsouris 75,114,001 (48.8, 2.33)**	630	
Bordeaux	Bordeaux- Merignac Airport 33,281,001 (44.83, −0.69)*	837	
Bilbao	Bilbao Airport, 1082(43.3, −2.9)*	1121	10 min
Santiago	Santiago EOAS (42.87, −8.54)	1573	

*Climate stations in airports **Centennial stations **1 ERA5 grid location slightly different.

environments with high temporal resolution. It can simulate overland flow dynamics, losses due to infiltration, depression storage and evaporation (derived using temperature data) and various retention and SUDS components (for detailed equations, refer to SWMM hydrology manual, Rossman and Huber 2016).

Two street scenarios are considered in this study to compare the runoff behaviour of conventional, heavily sealed urban street surfaces and the reduction potential of street surfaces modified with SUDS components between stations along the climate transect. The first scenario, as a default scenario, is a 'fully sealed' urban asphalt street with a length of 100 m, a width of 7 m and concrete sidewalks of 1.5 m on either side (Figure 2). For the second scenario, a pilot study was undertaken to assess reduction potential from a wider range of SUDS components including permeable pavement, block pavers, bio retention cells and rain gardens along the sidewalks of the street. As seen in previous SWMM modelling studies (Abdalla et al. 2021; Funke and Kleidorfer 2024), all SUDS components resulted in a significant reduction of runoff with reduction efficiency varying between 30% and 80% (Ahmad et al. 2025; Arvand et al. 2023). Block pavers are the SUDS measure, which can be most easily retrofitted to sidewalks and at the same time provide reasonable overland flow reductions. Therefore, the

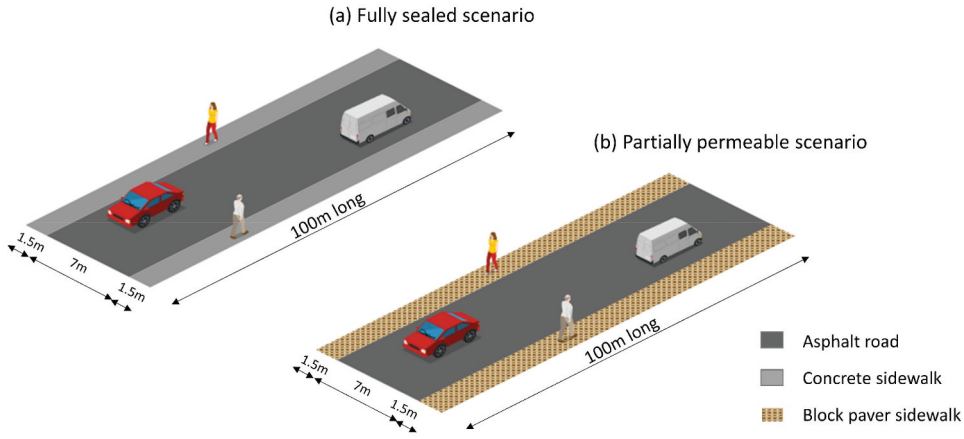

Figure 2. Schematic diagram of the two scenarios of urban street used to generate overland flow for the 10 cities.

second scenario of this study is a partially permeable urban street surface, with the same length and road width as scenario 1 and block pavers over the sidewalks on both sides. The longitudinal slope for both scenarios was set uniformly to 1%.

The parameterisation of the depression storage of the asphalt road in both scenarios was not trivial. Depression storage is, besides infiltration and evaporation losses, the most important filter to sequester overland flow rates from rainfall rate. Studies show that the depression storage varied between 0.1 and 5 mm for sealed surfaces such as cobblestone or block pavement (Haacke 2022; Nehls, Menzel, and Wessolek 2015) and 1–2 mm for asphalt surface (Hollis and Ovenden 1988). A pilot study evaluated the impact of varying depression storages (1 mm, 2 mm, 5 mm and 10 mm) on modelled overland flow for the fully sealed scenario (Appendix I Table A1). It was seen that runoff coefficients varied slightly for depression storages of 1 and 2 mm and decreased significantly with that of 5 and 10 mm. Assuming our hypothetic asphalt roads to be neither perfect nor ragged, and following the recommendation of SWMM User's Manual between 1.2 and 2.5 mm, a depression storage of 2 mm was selected for both scenarios. The infiltration rates and Manning's coefficients of asphalt road and concrete sidewalk were derived after Raimbault et al. (2002) and Yen (2001) respectively (Appendix II Table B1). The block paver setup includes four layers: a surface layer, a pavement layer, a soil layer and a storage layer (infiltration and storage parameters in Appendix II Table B1). SWMM calculates the daily evaporation loss with the Hargreaves method (Hargreaves and Samani 1985) using the daily maximum and minimum temperature and uniformly downscales it to the sub-hourly scale. Considering this limitation of SWMM, users may preferably use sub-daily evaporation data, if available.

Simulations were set up to run continuously over the entire investigation period (2012–2021). To avoid discrepancies due to the different temporal resolutions of the rainfall data, the 1 min and 6 min rainfall data from the German and French stations were aggregated to a 10 min resolution for computing overland flow events (objective 1). To analyse temporal scaling, the best available temporal resolution was employed for each city (objective 2). Overland flow events from the ERA5 data were compared with those using the best temporal resolution for each city (objective 3). For all three objectives, an overland flow computation and a reporting time step of 1 min were used in the SWMM.

2.3. Classification of overland flow events

To enable a quantitative comparison of overland flow occurrences among the 10 cities, a categorisation method needs to be applied to group them into small, medium, and large events. However, no formal method exists for classifying the overland flow. Traditionally, runoff events have been grouped into mean flow (Q50), (extremely) high flow (e.g. Q80, Q90 or Q95) and low flow (e.g. Q5, Q10) conditions (Rahimi, Deidda, and De Michele 2021; Zaherpour et al. 2018). Grouping based on discharge is not feasible here, because overland flow events on street surfaces are distinctly separate. Instead, we employed a percentile approach as used in the classification of rainfall events by Brieber and Hoy (2019), Schär et al. (2016). In a first step, individual runoff events were delineated from the simulated overland flow time series of the default scenario 1 (fully sealed) using the R-CRAN package 'IETD' (Duque 2020), adopting a three-hour inter-event time. Overland flow amounts were expressed in millimetres (equivalent to mm/m^2) throughout the study. The 50th and 80th percentiles of the total flows of all events from fully sealed scenario of all cities were calculated (all cities SC1 in Figure 3) and employed to categorise small events (<50th percentile, <4 mm), medium events (>50th and < 80th percentile, 4–11 mm) and large events (>80th percentile, >11 mm). To ensure comparability, the same magnitude delineations were used for scenario 2.

In order to analyse the statistical similarity of total flow and peak flow distribution of the 10 cities, the Tukey Honest Significant Differences method, known as Tukey's HSD test was conducted at a 95% confidence level using basic R functions TukeyHD() and aov(). The test allows multiple pairwise comparisons between the 10 cities and helps identify cities

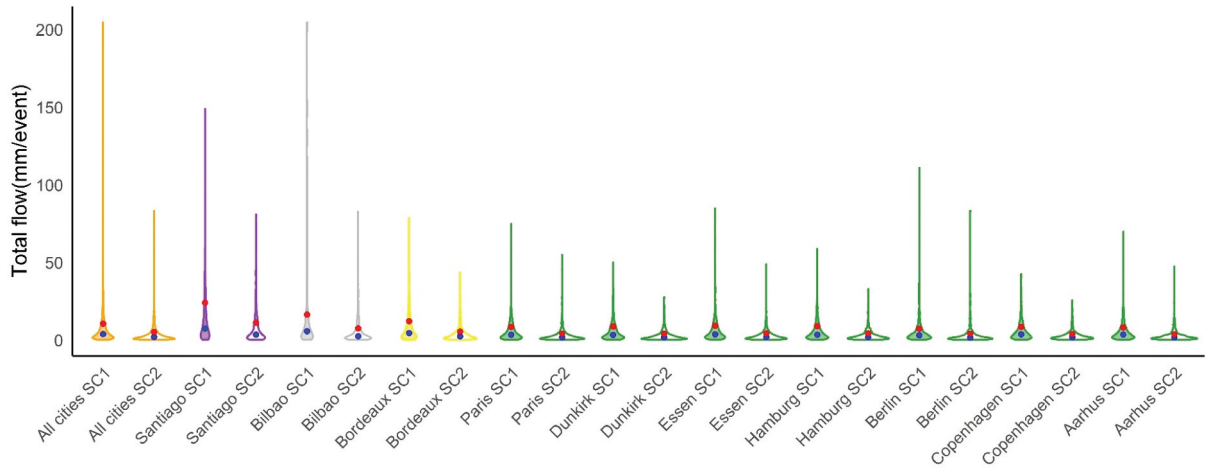

Figure 3. Total flow distribution of overland flow events (during 2012–2021) of the 10 cities across the transect combined ('All cities' in left end) and grouped by individual cities (Santiago de Compostela to Aarhus) for fully sealed, SC1 (colour-filled plot) and partially permeable, SC2 (colour-outline plot) scenarios. The blue and red points represent the 50th and 80th percentiles, respectively, for each violin plot.

with statistical similarities and dissimilarities. The test results are discussed in Section 3.1.

2.4. Concurrency of long dry spell with large runoff

Dry spell may be defined as a period of consecutive days without rainfall or with very little rainfall below a certain threshold, e.g. 0.1 mm in the study by Breinl et al. (2020) or 1 mm in the study by Bichet and Diedhiou (2018) to consider rainfall measurement errors or loss, for example, due to evaporation. We adapted their definitions by defining a dry spell as all consecutive days for which no overland flow was generated for the fully sealed scenario. Thus, we indirectly considered rainfall losses due to the effects of evaporation, infiltration and depression storage, as simulated by the SWMM model. Based on this definition, an R function was developed in order to identify the dry spells from the overland flow time series. Dry spells with a minimum length of 14 days were chosen for further analysis.

Previous studies by Qiu et al. (2021) and Santos et al. (2016) on the concurrency of long dry spells with rainstorms focused solely on the first rainfall event immediately at the end of the dry spell. In doing so, they may have missed concurrent events with some major rainstorms that occurred only hours after the first rainfall event. A pilot study undertaken looking into the overland flow events following long dry spells (>14 days) in the 10 European cities showed two cases of concurrency of long dry spells followed by overland flow: the first case named 'immediate overland flow' is the one aforementioned, where an overland flow event happens right at the end of a long dry spell (Figure 4(a)). In the second case, a small overland flow occurs marking the end of a dry spell, and within a day, a large overland flow event with significant peak flow occurs, which is named as 'lagged large overland flow' (Figure 4(b)). All of the

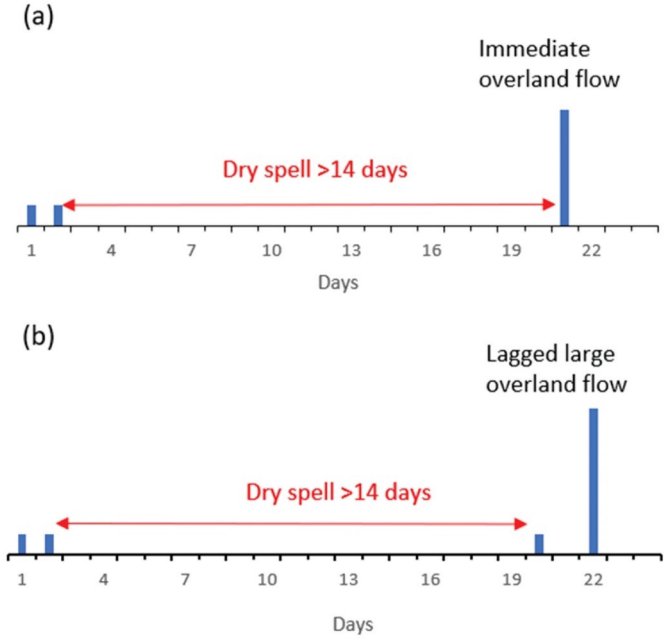

Figure 4. Definition of the two cases of concurrency of long dry spell with overland flow. (a) Immediate overland flow, (b) Lagged large overland flow.

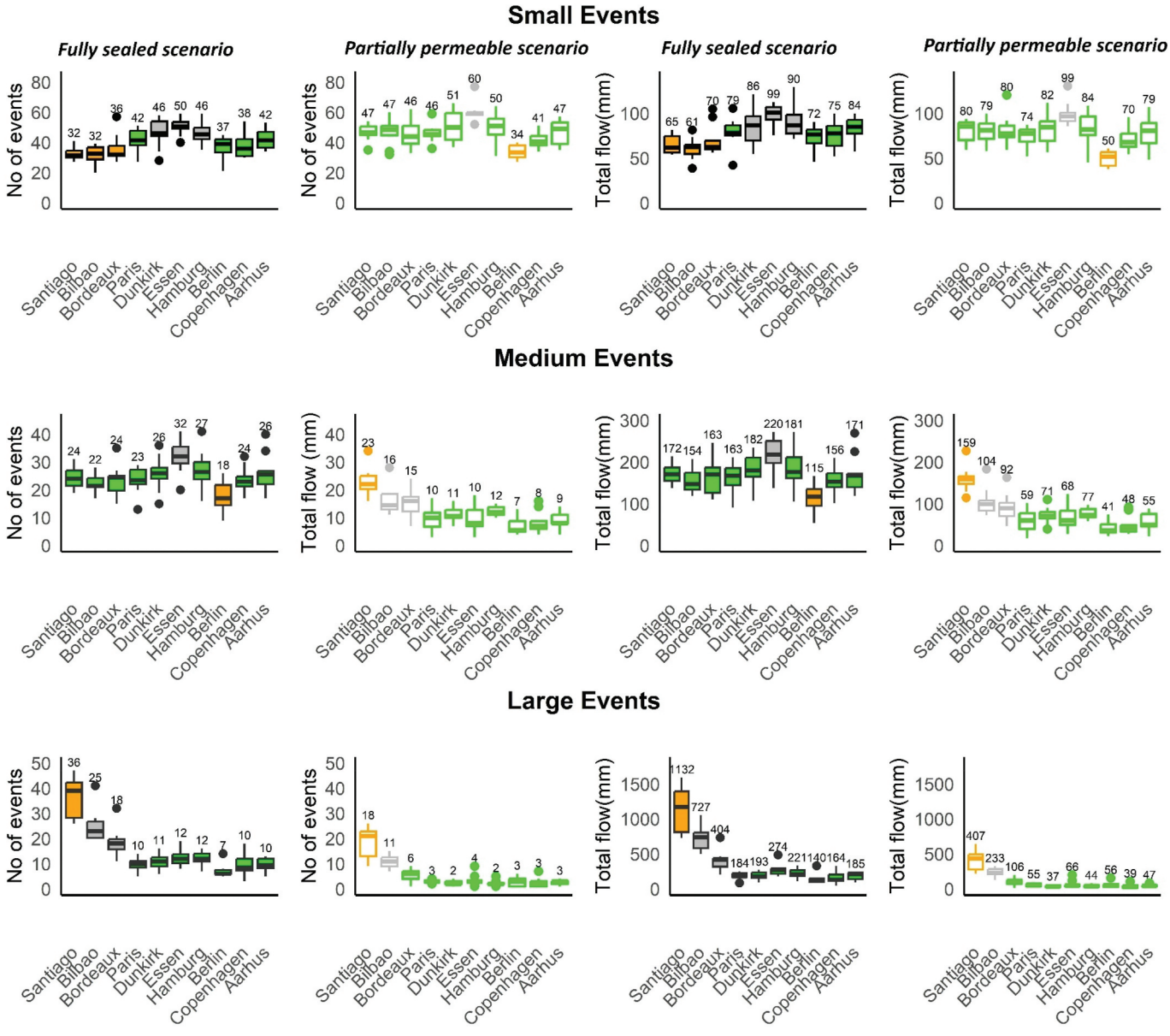

Figure 5. Comparison of the annual average number and total flow of overland flow characteristics classified into small (< 4 mm), medium (4–11 mm) and large events (>11 mm) of the 10 European cities for fully sealed (filled box plot) and partially permeable (outline box plot) scenarios. The colour of box plot represents the statistical similarity between the cities obtained through Tukey's HSD test and number at the top of box plot gives the annual mean value.

concurrency events were identified from the overland flow series using a simple filter routine scripted in R Cran, identifying each concurrency event and summarising its flow characteristics, the corresponding duration of the antecedent dry spell and the type (immediate or lagged) of concurrency.

3. Results

3.1. Comparison of overland flow behaviour of the 10 European cities

Over the time period–2012–2021, the annual frequency and total flow of medium overland flow events were found to be in the same range across the transect, with mean values ranging between 22 and 27 events per year and a total flow of 154–182 mm, respectively (Figure 5), with some minor deviations observed for the cities of Berlin and Essen. For the small events, the annual frequency and total flow varied moderately across the transect, with mean values ranging between 32 and 50 events per year and total flows of 61–99 mm, and the three groups of cities (represented in three colours in Figure 5) exhibiting statistical similarity. Regarding large overland flow events, both the annual frequency and total flow of the two most western cities, Santiago and Bilbao (25–36 events per year, 727–1132 mm), were significantly larger than those from the other cities (7–18 large events per year and total flow of 184–404 mm). This similarity was supported by Tukey's HSD test performed for pairwise comparisons of annual frequency and total flow (Figure 5).

For the partially permeable scenario, we see a clear reduction potential for all stations across the transect but with different characteristics. The annual frequency and total flow

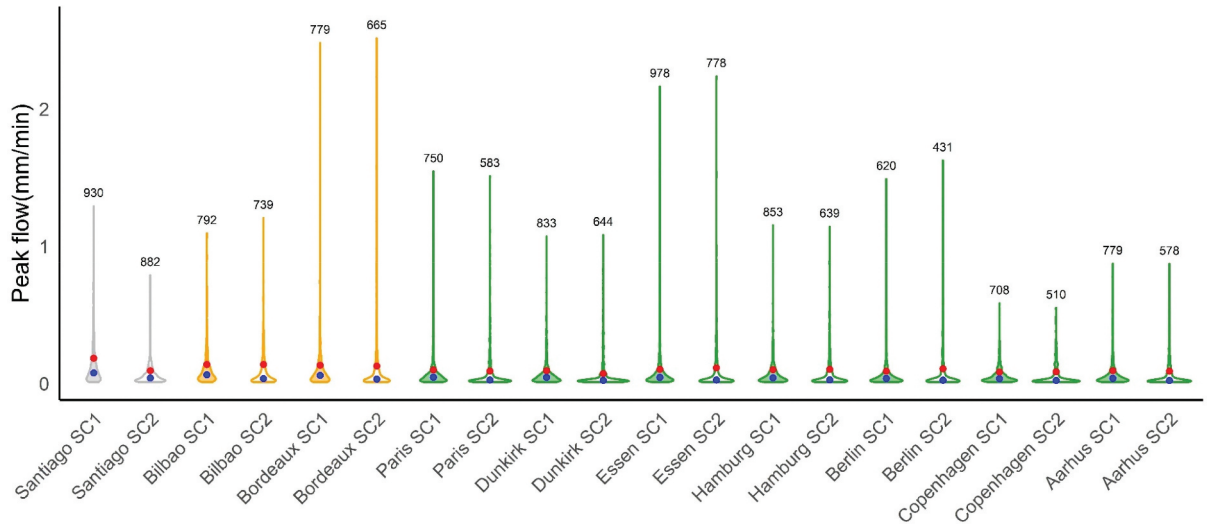

Figure 6. Peak flow (mm/min) distribution of overland flow events visualised as violin plots for the 10 cities across the transect (Santiago to Aarhus) for fully sealed (SC1, colour-fill plot) and partially permeable (SC2, colour-outline plot) scenarios. The distribution of cities which are statistically similar are represented with same colour. Blue and red circles represent the 50th, 80th percentiles of the respective violin plot; total number of events given on top of each violin.

of large events are drastically reduced for all cities (3 to 18 events per year), whereby the seven eastern cities of the transect exhibit an event and flow reduction of around two-third and three-fourth, respectively. The reduction is less pronounced for the western stations. A similar pattern is detected for the medium events, with a reduction of around two-thirds for annual frequency and flow for the eastern station, but only a slight or no reduction for the three western stations. The annual frequency and total flow of small events in the partially permeable scenario is higher compared to fully sealed scenario for all stations, since many of the events that were previously categorised as medium or large events in the fully sealed scenario were reduced to small events.

A temporal trend in the frequency and total flow of events could not be inferred as the extent of the study period was too short.

The distribution of the peak flows was characterised by median flows ranging between 0.02 and 0.076 mm/min considering both fully sealed and partially permeable scenarios. The median peak flows for both scenarios are in close range across the transect (Figure 6). Bordeaux and Copenhagen exhibited the largest and smallest individual peak flows at 2.5 mm/min and 0.75 mm/min, respectively. Tukey's HSD test performed for pairwise comparison of the peak flow distribution among the 10 cities showed statistical similarity for the seven cities from Paris to Aarhus (green violin plots in Figure 6) and Bilbao and Bordeaux (orange violin plots). The violin plot of the seven eastern cities has a significant level-bottomed shape, especially for the partially permeable scenario showing more frequent low-peak flow events compared to the remaining three western cities.

The same relationship regarding statistical similarity holds true for the distribution of the total flow of individual events along the transect (Figure 3).

The total flow-duration-peak-seasonality (tfdps) relationships (Figure 7) of the overland flow events for both scenarios of the 10 cities showed two distinct patterns changing from west to east. The first pattern, dominating the more western cities, is characterised by long-duration, large winter flow events (total flow >11 mm), with approximately 70% of total overland flow occurring in the winter and autumn months and no heavy summer events in both scenarios. However, between the two scenarios, the first pattern varies slightly with fewer long duration, large winter flow events for partially permeable scenario compared to fully sealed one

The second pattern, describing predominantly the seven eastern cities, is characterised by short duration, high peak flow events occurring in the three summer months, long duration, low peak flow events in the winter months and spring and autumn events assembled in between these two fringes regarding both peak and duration. The summer peaks are particularly pronounced in the cities of Paris, Essen and Berlin. Again, between the two scenarios, the second pattern varies with much fewer low peak winter events for the partially permeable scenario.

The tfdps relationship for Bordeaux exhibits a transitional form between the two patterns.

All cities experienced long dry-spells (>14 days) at least once a year, with maximal dry-spell durations varying between 30 and 50 days (Figure 8). The mean annual number of concurrency events varies from 3 to 5, with three occurrences per year in most cities.

High total and peak flows preceded by a long dry spell were particularly pronounced in the summer seasons in Berlin and the spring to autumn seasons in Santiago, Bilbao and Bordeaux (Figure 8) for both scenarios. For example, in Berlin, a long dry spell of 18 days in summer was followed by an event with a total flow of 28 mm and a peak of 1.1 mm/min. A minimum of 10% of the total number of concurrency events in the four

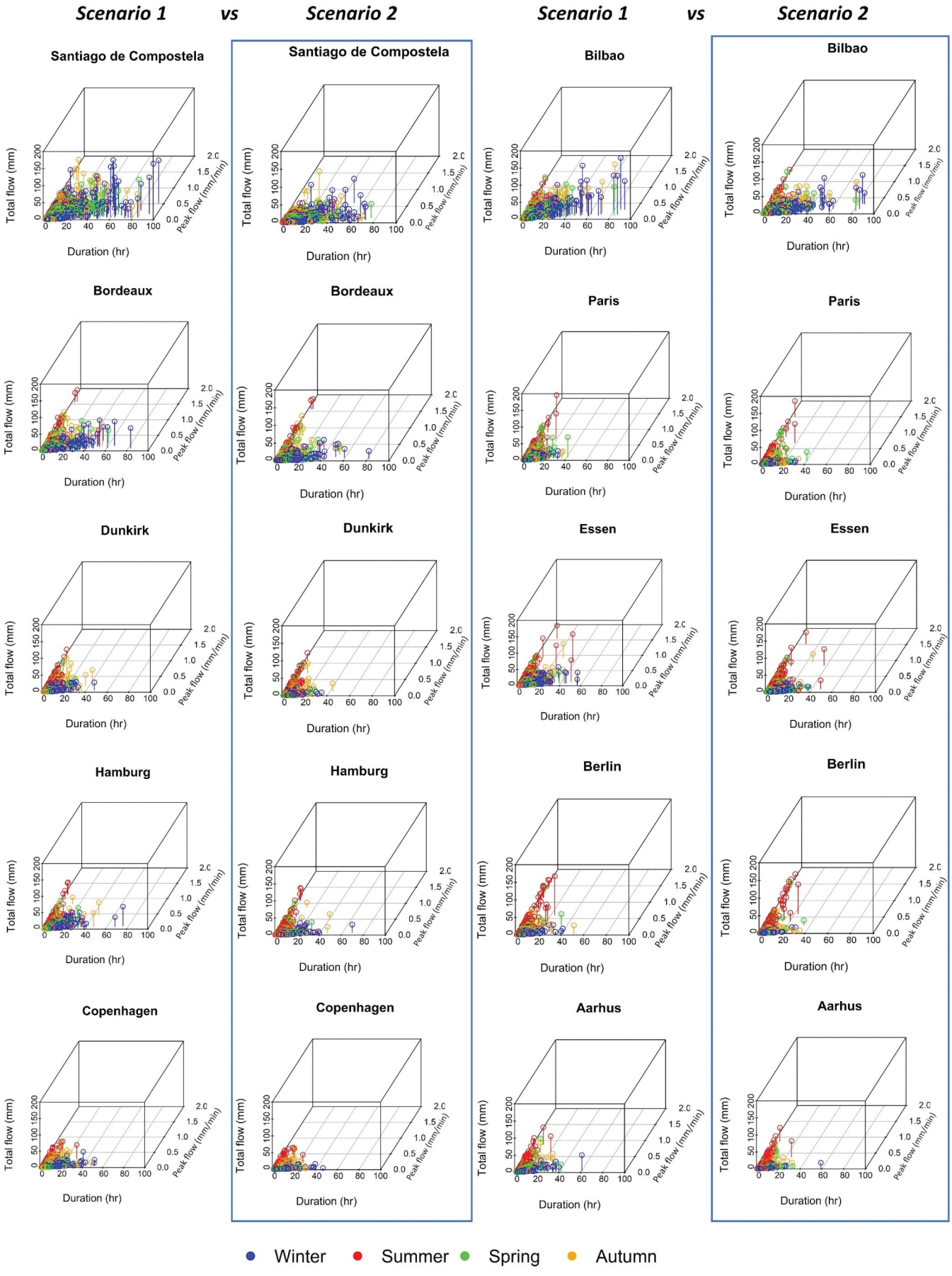

Figure 7. Total flow-duration-peak flow relationship of the overland flow events of the 10 European cities over the time period 2012–2021 for Scenario 1 (fully sealed scenario) and Scenario 2 (partially permeable, blue outline). Each point with its tail represents an individual event and the colour represents the season in which the event is happening.

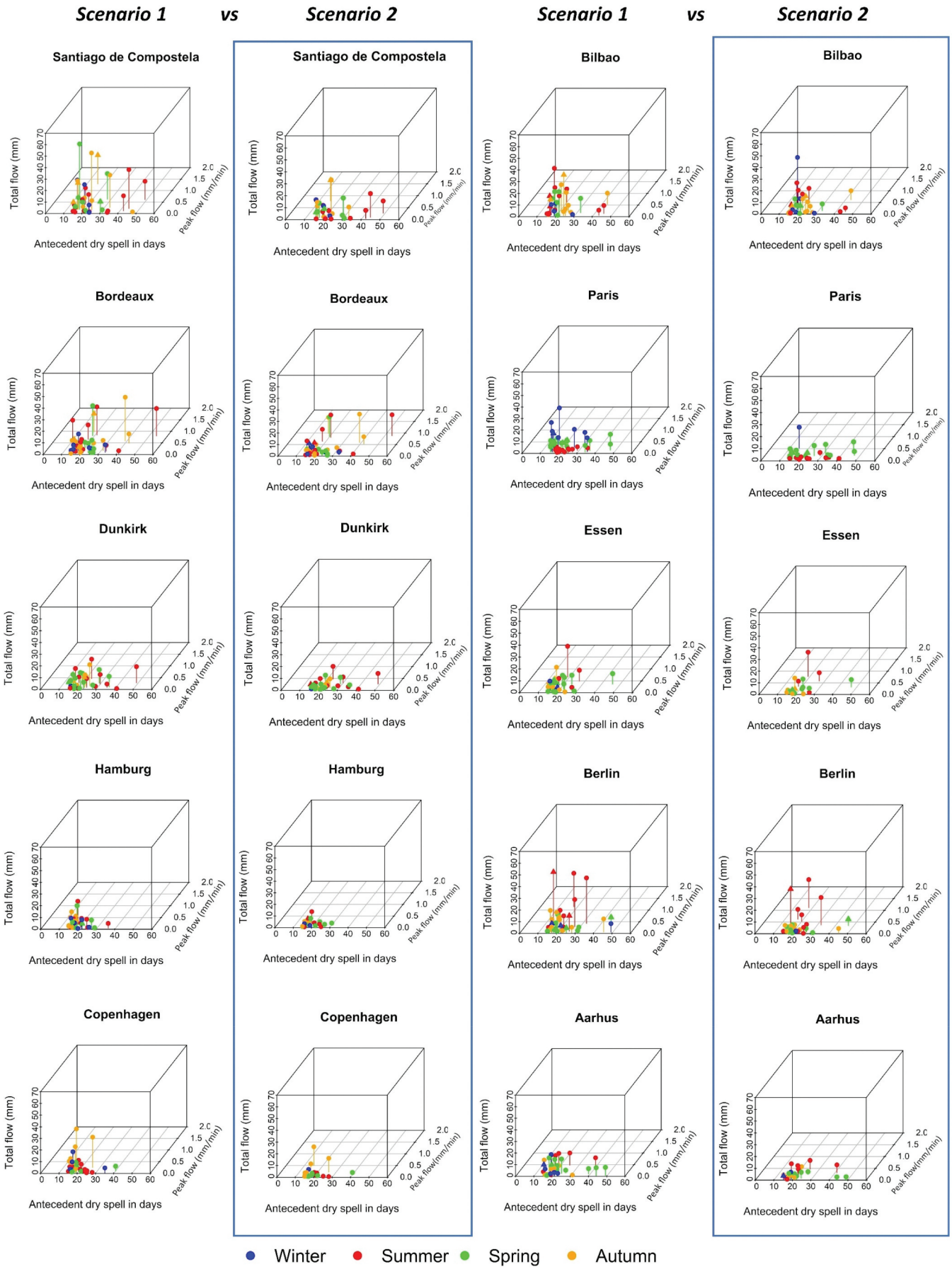

Figure 8. Concurrency of long dry spells followed by a rainstorm: Overland flow characteristics of events concurrent to long dry spell (duration larger than 14 days) for Scenario 1 (fully sealed) and Scenario 2 (partially permeable, blue outline) of the 10 European cities. The two cases 'immediate' and 'lagged' overland flow events (Figure 4) are represented with circle and triangle heads, respectively.

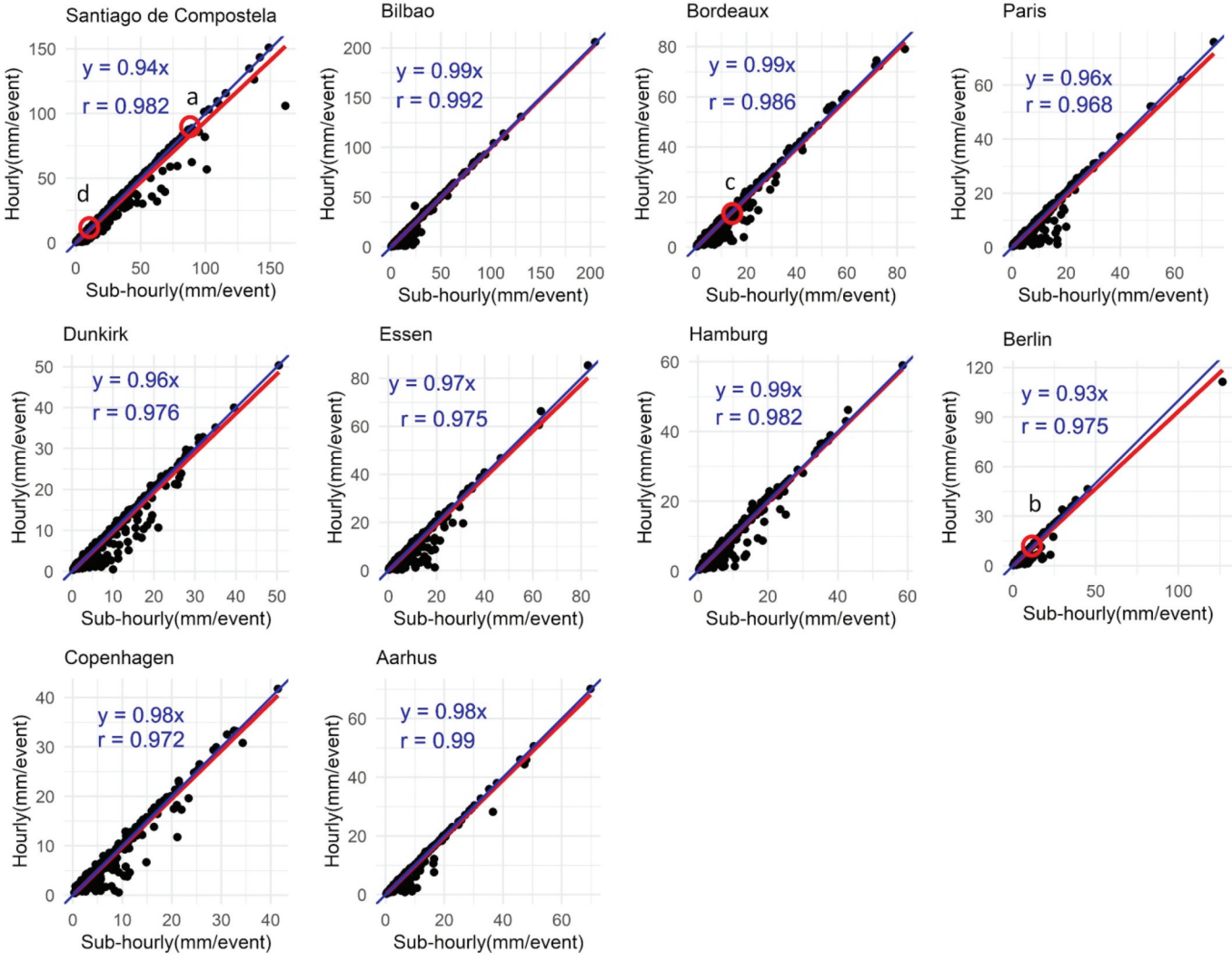

Figure 9. Comparison of total flow (mm/event) of the overland flow events during 2012–2021 computed for the fully sealed scenario using high resolution (x axis) and hourly rainfall data (y axis) of the 10 European cities. The linear regression model and the Pearson correlation coefficient (r) are shown in each scatter plot with the red line representing the regression line. The blue line is a 45 degree (1:1) line.

aforementioned cities came under the group 'lagged' large overland flow (depicted with a triangle head in Figure 8) with Berlin and Santiago having around 17% of its concurrency events under this group. Comparing the two scenarios, these four cities experience reduction in large concurrency events for the partially permeable scenario.

For the north-easternmost cities on the transect, Hamburg, Copenhagen and Aarhus, only moderate total and low peak flow events were recorded in any season after the dry spells for both scenarios. The 'lagged' large overland flow (depicted with a triangle head in Figure 8) is seldom observed in these three cities. There is no significant difference in concurrency events between the two scenarios for these cities. Concurrent events in Paris, Dunkirk and Essen were characterised by the comparably moderate total and peak flows. In Paris, around 17% of the concurrency events came under the 'lagged' large overland flow.

The antecedent dry period-total flow-peak flow relationship (Figure 8) shows that the magnitude and intensity of the overland flow did not increase with the duration of the dry spell.

3.2. *Effect of temporal scaling of sub-hourly to hourly rainfall data on overland flow generation across the European transect*

A comparison of overland flow computed with sub-hourly (1 min to 10 min, Table 1) rainfall data with overland flow computed with hourly rainfall data for the default 'fully sealed' scenario showed that the total overland flow of the events did not vary significantly for the 10 cities; the effect was consistent across the entire transect (Figure 9). For all cities, a linear regression model with slope close to 1 (0.93 to 0.99) and strong Pearson correlation coefficients (0.96 to 0.99) was evident between total flow (mm) of individual events obtained with sub-hourly and hourly rainfall data. However, the peak flow of events was consistently underestimated with the usage of hourly resolution data that the

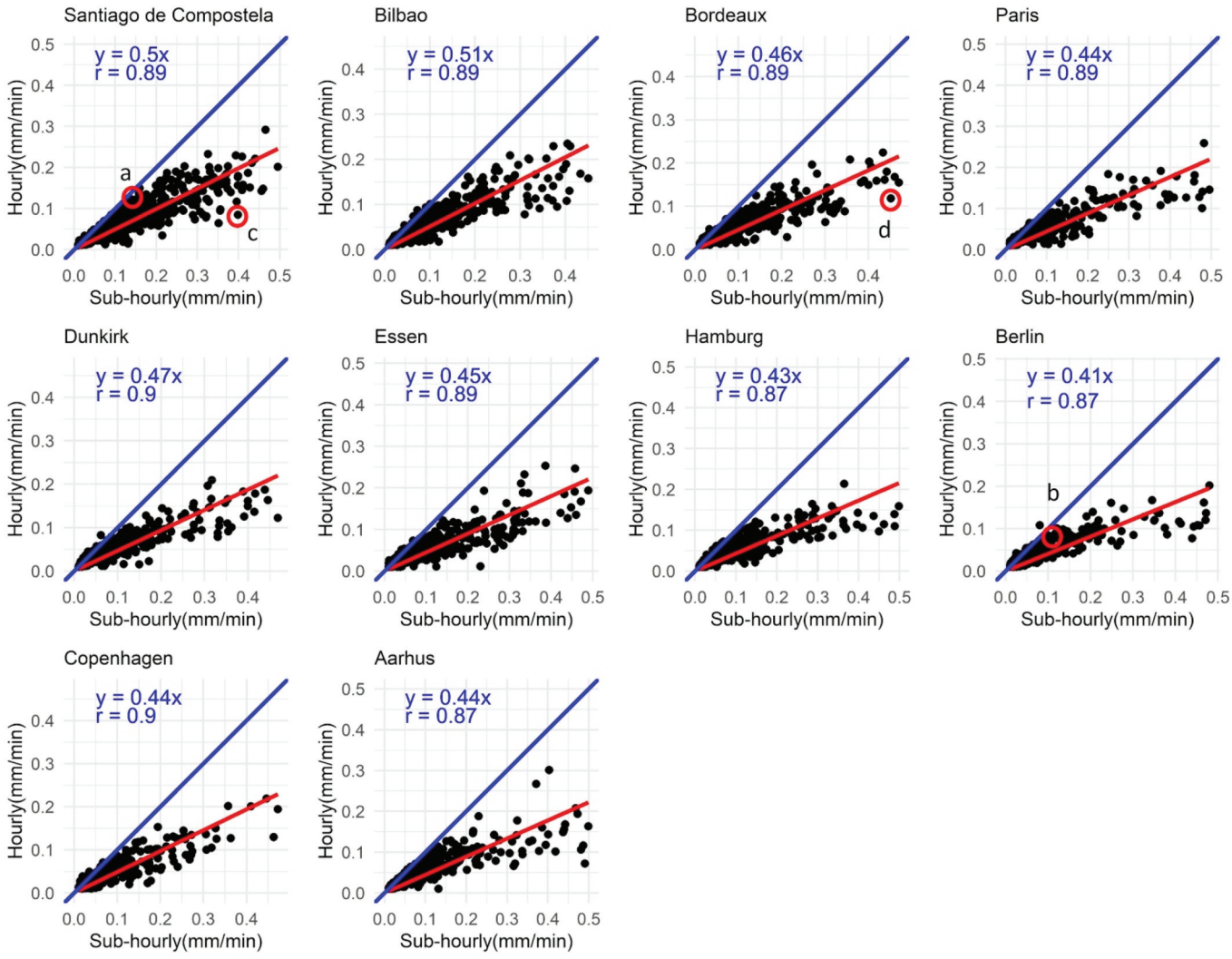

Figure 10. Comparison of the peak flow (mm/min) of the overland flow events during 2012–2021 computed for the fully sealed scenario using sub-hourly (x axis) and hourly rainfall data (y axis) for the 10 cities. The linear regression model and the Pearson correlation coefficient (r) are shown in each scatter plot with the red line representing the regression line. The blue line is a 45 degree (1:1) line; individual hydrographs of events a to d, marked with red circles, are depicted in Figure 11.

linear regression model gave slope around 0.5 (0.41 to 0.51) for the 10 cities (Figure 10).

In general, temporal scaling from sub-hourly to hourly resolution works well with longer events characterised by average peak flow and total flow, as marked with data points a and b in Figure 10, whose hydrographs are shown in Figure 11. Hourly data did not reproduce overland flow events well for short-duration high-peak flow events, marked as data points c and d in Figure 10 and corresponding hydrographs in Figure 11, for which peak flow was underestimated by 63% and 67%, respectively.

3.3. ERA5-land data as a proxy for high-resolution data for overland flow analysis across the European transect

A comparison of event-based total overland flows generated using sub-hourly rain data (1–10 min, Table 1) with overland flows generated by hourly ERA5-Land rainfall for the default 'fully sealed' scenario data showed that the majority of the cities had a regression slope close to 1 (Figure 12). However, the correlation coefficients were very weak for Santiago (0.14), strong for Bilbao (0.67) and Berlin (0.74) and moderate for all the other cities (0.51 and 0.58) (Figure 12).

Figure 13 shows several hydrographs calculated using sub-hourly and aggregated hourly station rain data and hourly ERA5-land rain data. Data point a in Figures 12 and 13(a) depicts a long-duration, low peak flow overland flow event, which is reproduced well by the ERA5-land data with regard to timing, peak and total flow. The three remaining hydrographs show distinct faulty patterns and explain the loss of correlation, which can be attributed to several misrepresentations of the ERA5-land rain data, resulting in both overestimation and underestimation of peak and total flows (data points b and c in Figures 12 and 13(b,c)) or a considerable lag of the event (data point d in Figures 12 and 13(d)).

The inconsistency of ERA5-land-driven simulations in comparison with the station data was apparent across the transect, with Santiago's overland flow reproduction being particularly poor. The comparison of the peak flow is not shown because the previous section already showed that peak flow is heavily

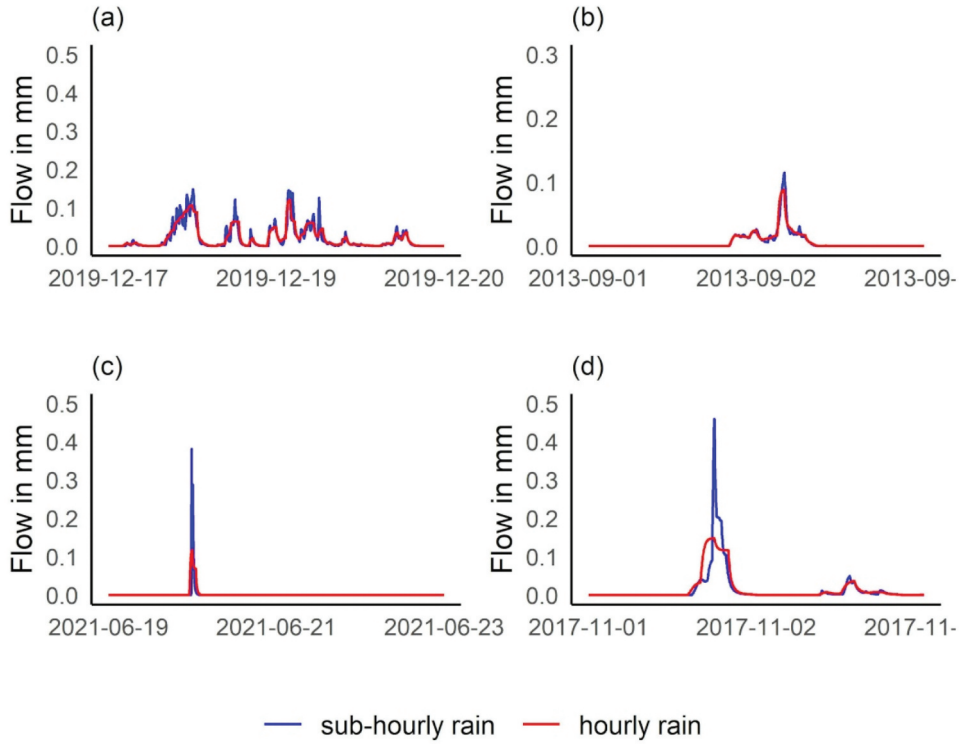

Figure 11. Flow hydrograph of events computed with high resolution, sub-hourly rainfall (blue) and 1-hour resolution rainfall (red) for (a) Santiago de Compostela, (b) Berlin, (c) Bordeaux and (d) Santiago de Compostela. Exemplary temporal scaling effects are shown for long duration, average peak flow events are shown in the top row and for short duration, high peak flow events in the bottom row.

underestimated when using hourly rather than sub-hourly resolutions.

4. Discussion

4.1. Similarity assessment of overland flow dynamics and its relevance for diffuse pollution

The comparison of several attributes of overland flow dynamics of two urban street scenarios for 10 cities along a European transect showed mostly similar behaviour, but some distinct differences in overland flow attributes. A clear similarity exists in the annual frequency and total flow of medium-to-large events, total and peak flow distribution and tdfps relationship of overland flow events in both scenarios for all cities along the transect, except those at the western end, which showed a large number of extreme events and different tdfps patterns. Comparison between the two scenarios suggests that introducing SUDS components reduces large and medium events, particularly the low peak winter events, more pronounced for the north-eastern and central cities of the transect. Hence, SUDS measures do not as effectively reduce medium-to-large events in the western part of the transect. A similar number of approximately three to five concurrent large runoff events with long dry spells (greater than 14 d) were identified for the 10 cities. However, the corresponding total and peak flows differed clearly between the cities, with some cities, such as Berlin, characterised by much larger and flashier concurrency events, whereas the more northern stations yielded mostly moderate and low peak flow events concurrent with a long dry spell. A reduction in these large and flashier concurrent events is observed with the introduction of SUDS. The combined findings of overland flow dynamics, seasonality and concurrency partly support the initial hypothesis that cities in the same climate zone exhibit similar overland flow dynamics.

The anomalies observed in the cities at the western end of the transect could be attributed to the influence of the neighbouring Mediterranean climate zone (Csb, as in Rubel et al. 2017; see Figure 1 for the spatial distribution of climate zones). Whitford et al. (2023) found a clear disparity in rainfall extremes, which were more pronounced and frequent in the Csb zone compared to the Cfb zone. Other spatial representations (Beck et al. 2018; Kottek et al. 2006) of climate zones also include Santiago de Compostela in the Csb zone rather than Csb zone, which could further explain the apparent discrepancy in overland flow behaviour at the western end of the transect.

Previous studies that compared overland flow across European cities focused on extreme overland flow or pluvial flooding in urban areas using a design storm of minimum 10-year return period. For this purpose, Essenfelder et al. (2022) developed probabilistic pluvial flood hazard mapping for 20 European cities to derive the pluvial flooding depth and spatial extent as a function of extreme rainfall. Similarly, Guerreiro et al. (2017) used a hydrodynamic model to simulate pluvial flooding in 570 European cities for a 10-year design storm, and compared the percentage of flooded areas between the cities. The similarity in large events found across this transect in this study is consistent with Guerreiro et al. (2017), who obtained rainfall extreme values and percentages of flooded areas in close range in the studied climate zone.

To the best of our knowledge, no previous study has aimed to understand the overall overland flow behaviour, not only the

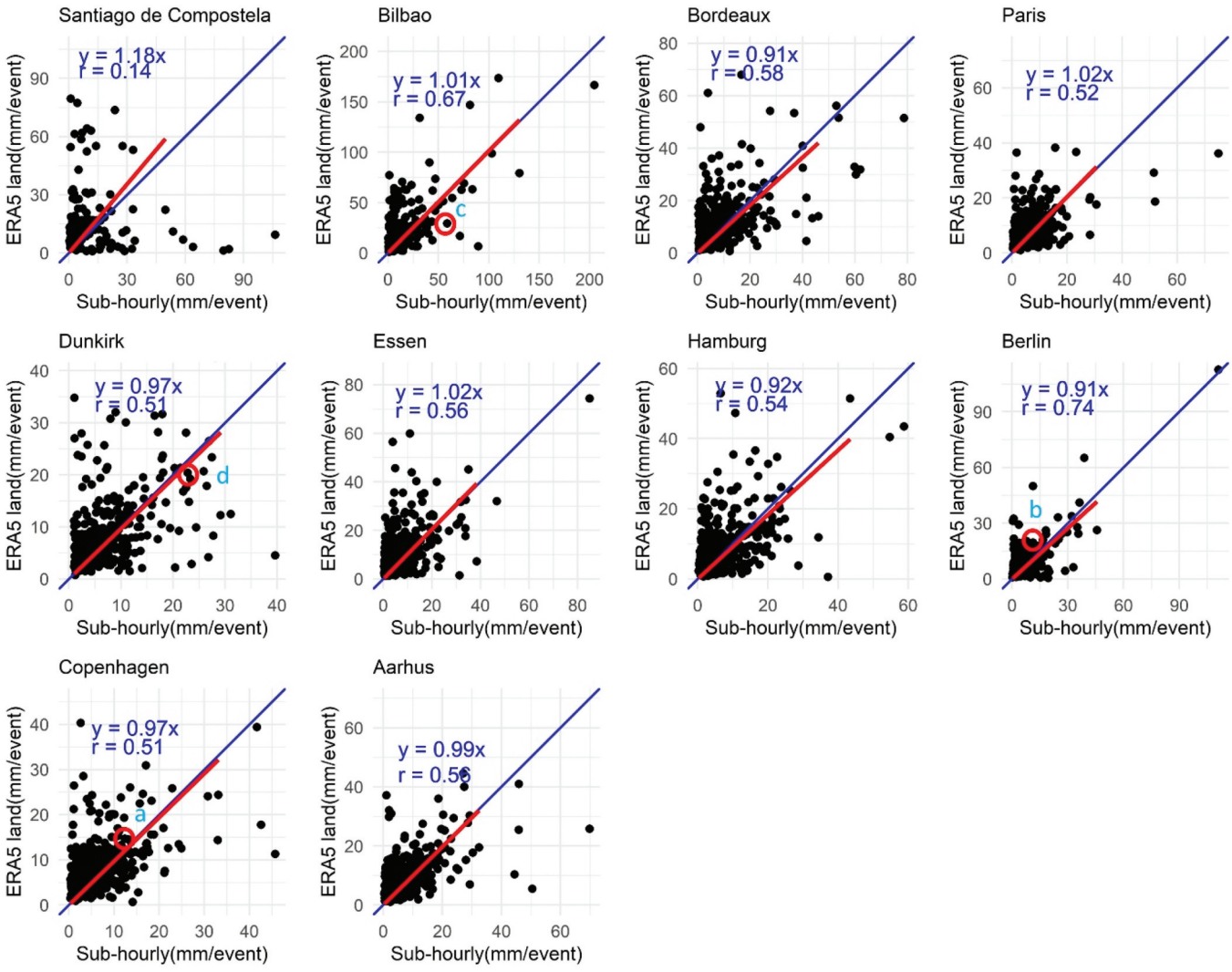

Figure 12. Comparison of the total flow (mm/event) of overland flow events during 2012–2021 computed for the fully sealed scenario with sub-hourly station data (x axis) and ERA5-Land rainfall data (y axis) for the 10 cities. The linear regression model and the Pearson correlation coefficient (r) are shown in each scatter plot with the red line representing the regression line. The blue line is a 45 degree (1:1) line, individual hydrographs of events a to d, marked with red circles, are depicted in Figure 13.

extreme one, or the resulting diffuse pollution and CSO loads across Europe. Relevant for diffuse pollution loads and CSO spills, the two here identified tdfps patterns across the transect imply two pollution transport modes: short, high-peak flow summer events in the middle and eastern parts of the transect and long, large flow autumn to winter events at its western end. The higher number of large events suggests a greater potential for diffuse pollutants to reach the waterbodies at the western end of the transect. Because the resulting CSO spills strongly depend on local site conditions, such as topography, degree of sealing and the design of the existing drainage network, a generalisation of the two transport modes and the resulting impacts on surface water quality cannot yet be drawn. A full interpretation of the pollutant transport potential of overland flow requires an immense dataset of water quality series in urban settings, which is currently not available to the extent required.

This study showed the prevalence of long dry spells followed by large rainstorms across the European transect, suggesting their critical role in diffuse pollution from urban surfaces after long accumulation times. Previous studies undertaken to understand the impact of these long dry spells on runoff quality were mostly field studies restricted to a year of data collection (Wang et al. 2020 in Germany; Li and Barrett 2008 in the USA). Only a few studies exist that looked into rain events preceded by long dry spells (longer than 14 days) which were found in this study to occur frequently in all cities (Soltaninia et al. 2023 in Iran; Kim et al. 2018 in the USA; Murphy, Cochrane, and O'Sullivan 2015 in New Zealand). The study also showed that the magnitude and intensity of concurrent runoff events are not proportional to dry spell duration, as runoff primarily depends on the rainfall that follows, which does not necessarily increase with longer dry spells. This contrasts the findings of Qiu et al. (2021) in rural catchments, where runoff is strongly influenced by antecedent soil moisture, which depends on dry spell duration. However, a full analysis of the effects of concurrency events, especially longer dry spells, on diffuse pollution transfer across Europe is still pending and is considered a crucial step in understanding the significance of concurrency events on surface water quality.

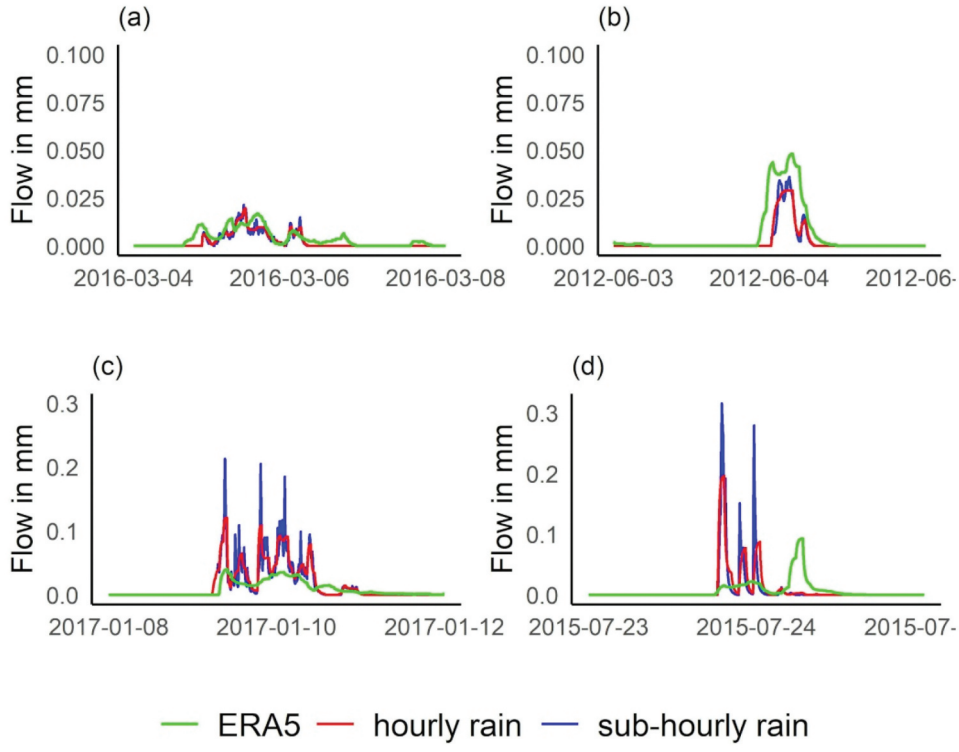

Figure 13. Examples of flow hydrographs of events computed with sub-hourly, hourly station data and ERA5-Land data for Copenhagen (a), Berlin (b), Bilbao (c), Dunkirk(d). (a) shows a good fit between the three-rain data, (b) illustrates an overestimation by ERA5-Land data, (c) illustrates an underestimation by ERA5-Land data and (d) represents a lagged occurrence of the entire event generated by ERA5-Land in comparison to station data.

4.2. Temporal scaling and data availability

The lack of availability of sub-hourly rainfall data remains a challenge. Open access to these data is possible only in a few EU countries or, alternatively, one must rely on local networks in order to obtain the data. By considering this limitation, the effects of temporal scaling of rain data from sub-hourly to hourly resolutions on overland flow generation were analysed and found to be consistent across the transect. These results are consistent with those of previous studies (Berne et al. 2004; Bruni et al. 2015) which found no effects of temporal scaling on the total overland flow or volume. However, the underestimation of peak flows with the hourly data set averaged to be 50% for all cities, mostly in response to convective rainstorms. Specifically, the peak flow rates determine diffuse pollutant wash-off and transport, flash flooding and CSO spills (Chowdhury, Egodawatta, and McGree 2023), the substitution of sub-hourly by hourly rain data to assess diffuse pollution rates is therefore limited.

ERA5-Land data were found to be a reasonable proxy for sub-hourly rainfall data for modelling total overland flow, except for poor correlations at the western end of the transect. This aligns well with Hassler and Lauer (2021), who found good agreement between station rain data and ERA5 data in Central Europe. The poor correlation in the western end is supported by the rainfall study by Rivoire, Martius, and Naveau (2021), which obtained poor agreement between the ERA5 land and gridded observation data in this region owing to the fewer number of observation stations. Apart from the limitation of its hourly resolution in predicting peak flow, ERA5-Land rain data have shortcomings such as reduced intensity of convective events (Chen, Dai, and Hall 2021) and an overestimation of low and medium precipitation (Gomis-Cebolla et al. 2023). Our findings indicate that these shortcomings are error-propagated in overland flows, such as the underestimation of large flows and overestimation of low and medium flows. Additionally, the limitation of comparing a station-based rain data with grid averaged ERA5 land data could also be attributed to errors.

4.3. Limitations and opportunities

Using two hypothetical urban street scenarios to compare overland flow dynamics across a European transect may appear oversimplified, as it primarily involves signal processing to transform rainfall into overland flow series. On the other hand, even on such a small spatial scale, the rainfall-runoff transformation is known to be highly nonlinear due to the various loss functions (depression, infiltration, evaporation) that show different markedness on different temporal scales. To compare the capacities of SUDS measures, the rainfall-runoff transformation becomes even more pronounced due to their increased infiltration losses and retention capacities. A full analysis could also include variations within and between cities in regard to slope, street conditions and different SUDS (beyond what was done in our pilot study) and information on the combined and separate sewer systems with different national design criteria, resulting in different susceptibilities to overland flow events. Finally, the fractions of urban drainage water being treated

and the frequency of CSO spills indicate the differences in overland flow and associated pollution patterns that impact surface water quality. However, considering many details of urban drainage networks, a comparison between a number of cities is a very complicated task.

This study compared overland flow events using high-resolution rainfall data and opened up a whole arena of new research questions regarding the functional connectivity of urban diffuse pollution (Paton and Haacke 2021), such as the analysis of different potential transport modes of diffuse pollution and the effects of long accumulation times during dry spells on pollutant supply. For a comprehensive analysis of these two fields, more field monitoring of runoff and pollutant magnitudes is required, a task that might be challenging to carry out across the entire EU transect of cities.

5. Conclusion

A comparison of overland flow behaviour across prominent climate zones in Europe suggests that cities in the same climate zone have similar overland flow dynamics, except for some disparities in large events and the tdfps relationship of overland flow events in western cities of the climate zone. The implementation of SUDS measures has a reduction potential of around two-thirds for medium and large events in the seven eastern cities of the transect. At the same time, the study showed that even cities in the same climate zone showed some disparities in their concurrent behaviour of runoff and long dry spells. Further analysis needs to be carried out to study the significance of concurrency events on diffuse pollution and water quality of receiving surface waters.

To define a better legal framework, other EU climate zones must also be investigated. This stresses the necessity of collating sub-hourly rainfall data from local sources to form an EU database, considering the limitations of hourly data in estimating the peak flow, which limits the reproduction of diffuse pollution and CSO spills. If sub-hourly rainfall data cannot be acquired from local sources, the ERA5 dataset can serve as a proxy for generating overland flow across Europe, although some limitations remain regarding its ability to reproduce convective events and low rainfall intensities.

Disclosure statement

No potential conflict of interest was reported by the author(s).

Funding

This work received funding from the European Union as part of WATERUN project within Horizon Europe programme under the Grant agreement [n° 101060922].

ORCID

Boney Anna Joseph http://orcid.org/0009-0004-8099-0696
Nasrin Haacke http://orcid.org/0000-0001-9065-729X
Eva Paton http://orcid.org/0000-0002-5619-9958

Data availability statement

The data used in the study are either open source or received upon request from meteorological offices, details of which are provided in Table 1. The sources are Danish Meteorological Institute – Open Data, DWD Climate Data Center, Meteo France Public data portal, State Meteorological Agency AEMET, Meteogalicia.

References

Abdalla, Elhadi M. H., Ingrid Selseth, Tone M. Muthanna, Herman Helness, Knut Alfredsen, Terje Gaarden, and Edvard Sivertsen. 2021. "Hydrological Performance of Lined Permeable Pavements in Norway." *Blue-Green Systems* 3 (1): 107–118. https://doi.org/10.2166/bgs.2021.009.

Ahmad, Shakeel, Haifeng Jia, Anam Ashraf, Dingkun Yin, Zhengxia Chen, R. Rasheed Ahmed, and Muhammad Israr. 2025. "Quantifying LID Impact: A Modified Metric for Enhanced Flood Mitigation and Urban Resilience." *Resources, Conservation & Recycling* 215:108089. https://doi.org/10.1016/j.resconrec.2024.108089.

Aronica, Giuseppe, Gabriele Freni, and Elisa Oliveri. 2005. "Uncertainty Analysis of the Influence of Rainfall Time Resolution in the Modelling of Urban Drainage Systems." *Hydrological Processes* 19 (5): 1055–1071. https://doi.org/10.1002/hyp.5645.

Arvand, Sedigheh, Zahra Ganji Noroozi, Mahdi Delghandi, and Akbar Alipour. 2023. "Evaluating the Impact of LID-BMPs on Urban Runoff Reduction in an Urban Sub-Catchment." *Urban Water Journal* 20 (5): 604–615. https://doi.org/10.1080/1573062X.2023.2207083.

Beck, Hylke E., Niklaus E. Zimmermann, Tim R. McVicar, Noemi Vergopolan, Alexis Berg, and Eric F. Wood. 2018. "Present and Future Köppen-Geiger Climate Classification Maps at 1-Km Resolution." *Scientific Data* 5 (1): 180214. https://doi.org/10.1038/sdata.2018.214.

Berne, Alexis, Guy Delrieu, Jean-Dominic Creutin, and Charles Obled. 2004. "Temporal and Spatial Resolution of Rainfall Measurements Required for Urban Hydrology." *Journal of Hydrology* 299 (3–4): 166–179. https://doi.org/10.1016/S0022-1694(04)00363-4.

Bichet, Adeline, and Arona Diedhiou. 2018. "West African Sahel Has Become Wetter During the Last 30 Years, but Dry Spells are Shorter and More Frequent." *Climate Research* 75 (2): 155–162. https://doi.org/10.3354/cr01515.

Breinl, Korbinian, Giuliano Di Baldassarre, Maurizio Mazzoleni, David Lun, and Giulia Vico. 2020. "Extreme Dry and Wet Spells Face Changes in Their Duration and Timing." *Environmental Research Letters* 15 (7): 074040. https://doi.org/10.1088/1748-9326/ab7d05.

Brieber, Annika, and Andreas Hoy. 2019. "Statistical Analysis of Very High-Resolution Precipitation Data and Relation to Atmospheric Circulation in Central Germany." *Advances in Science and Research* 16 (May): 69–73. https://doi.org/10.5194/asr-16-69-2019.

Bruni, Guendalina, R. Reinoso, N. C. Van De Giesen, F. H. L. R. Clemens, and J. A. E. Ten Veldhuis. 2015. "On the Sensitivity of Urban Hydrodynamic Modelling to Rainfall Spatial and Temporal Resolution." *Hydrology and Earth System Sciences* 19 (2): 691–709. https://doi.org/10.5194/hess-19-691-2015.

Chen, Di, Aiguo Dai, and Alex Hall. 2021. "The Convective-To-Total Precipitation Ratio and the "Drizzling" Bias in Climate Models." *Journal of Geophysical Research Atmospheres* 126 (16): e2020JD034198. https://doi.org/10.1029/2020JD034198.

Chowdhury, Anupam, Prasanna Egodawatta, and James McGree. 2023. "Pattern-Based Assessment of the Influence of Rainfall Characteristics on Urban Stormwater Quality." *Water Science & Technology* 87 (9): 2292–2303.

Chui, Ting F. M., Xin Liu, and Wenting Zhan. 2016. "Assessing Cost-Effectiveness of Specific LID Practice Designs in Response to Large Storm Events." *Journal of Hydrology* 53:353–364. https://doi.org/10.1016/j.jhydrol.2015.12.011.

Copernicus Climate Change Service. 2023. "ERA5-Land Hourly Data from 1950 to Present." Accessed July 25, 2023. https://cds.climate.copernicus.eu/cdsapp#!/dataset/reanalysis-era5-land?tab=form.

Danish Meteorological Institute- Open Data. 2023. "Meteorological Observation Data." https://confluence.govcloud.dk/display/FDAPI/Meteorological+Observation+Data.

DeMott, Charlotte A., David A. Randall, and Marat Khairoutdinov. 2007. "Convective Precipitation Variability as a Tool for General Circulation Model Analysis." *Journal of Climate* 20 (1): 91–112. https://doi.org/10.1175/JCLI3991.1.

Dos Santos, Julio Cesar Neves, Eunice Maia De Andrade, Maria João Simas Guerreiro, Pedro Henrique Augusto Medeiros, Helba Araújo De Queiroz Palácio, and José Ribeiro De Araújo Neto. 2016. "Effect of Dry Spells and Soil Cracking on Runoff Generation in a Semiarid Micro Watershed Under Land Use Change." *Journal of Hydrology* 541 (October): 1057–1066. https://doi.org/10.1016/j.jhydrol.2016.08.016.

Duque, L. F. 2020. "Inter-Event Time Definition (Package 'IETD')." https://cran.r-project.org/web/packages/IETD/index.html.

DWD Climate Data Center. 2023. "Historical 1-Min Station Observation of Precipitation." Accessed June 13, 2023. https://cdc.dwd.de/portal/.

ECMWF. 2023. "ERA5-Land Data Documentation." Accessed July 25, 2023. https://confluence.ecmwf.int/display/CKB/ERA5-Land%3A+data+documentation.

Essenfelder, Arthur H., Stefano Bagli, Jaroslav Mysiak, Jeremy S. Pal, Paola Mercogliano, Alfredo Reder, Guido Rianna, Paolo Mazzoli, Davide Broccoli, and Valerio Luzzi. 2022. "Probabilistic Assessment of Pluvial Flood Risk Across 20 European Cities: A Demonstrator of the Copernicus Disaster Risk Reduction Service for Pluvial Flood Risk in Urban Areas." *Water, Economics & Policy* 8 (03): 2240007. https://doi.org/10.1142/S2382624X22400070.

European Commission. 2014. "The EU Water Framework Directive." https://data.europa.eu/doi/10.2779/75229.

European Commission. 2022. "Proposal for a Directive of the European Parliament and of the Council Concerning Urban Wastewater Treatment." https://environment.ec.europa.eu/topics/water/urban-wastewater_en.

Fletcher, T. D., H. Andrieu, and P. Hamel. 2013. "Understanding, Management and Modelling of Urban Hydrology and Its Consequences for Receiving Waters: A State of the Art." *Advances in Water Resources* 51:261–279. https://doi.org/10.1016/j.advwatres.2012.09.001.

Funke, Fabian, and Manfred Kleidorfer. 2024. "Sensitivity of Sustainable Urban Drainage Systems to Precipitation Events and Malfunctions." *Blue-Green Systems* 6 (1): 33–52. https://doi.org/10.2166/bgs.2024.046.

Gomis-Cebolla, José, Viera Rattayova, Sergio Salazar-Galán, and Félix Francés. 2023. "Evaluation of ERA5 and ERA5-Land Reanalysis Precipitation Datasets Over Spain (1951–2020)." *Atmospheric Research* 284 (March): 106606. https://doi.org/10.1016/j.atmosres.2023.106606.

Guerreiro, Selma, Vassilis Glenis, Richard Dawson, and Chris Kilsby. 2017. "Pluvial Flooding in European Cities—A Continental Approach to Urban Flood Modelling." *Water* 9 (4): 296. https://doi.org/10.3390/w9040296.

Haacke, Nasrin. 2022. "Pilot Study: Depression Storage Capacities of Different Real Urban Surfaces Quantified by a Terrestrial Laser Scanning-Based Method." PhD Thesis, Technical University of Berlin. https://doi.org/10.14279/depositonce-16434.

Hargreaves, George, and Zohrab Samani. 1985. "Reference Crop Evapotranspiration from Temperature." *Applied Engineering in Agriculture* 1 (2): 96–99. https://doi.org/10.13031/2013.26773.

Hassler, Birgit, and Axel Lauer. 2021. "Comparison of Reanalysis and Observational Precipitation Datasets Including ERA5 and WFDE5." *Atmosphere* 12 (11): 1462. https://doi.org/10.3390/atmos12111462.

Hollis, G. E., and J. C. Ovenden. 1988. "The Quantity of Stormwater Runoff from Ten Stretches of Road, a Car Park and Eight Roofs in Hertfordshire, England During 1983." *Hydrological Processes* 2 (3): 227–243. https://doi.org/10.1002/hyp.3360020304.

Kawohl, Tobias Olliver. 2019. "Evaluation of ERA5, ERA5-Land, and IMERG-F Precipitation with a Particular Focus on Elevation-Dependent Variations: A Comparative Analysis Using Observations from Germany and Brazil." PhD Thesis, Univeristy of Hamburg. https://ediss.sub.uni-hamburg.de/handle/ediss/6194.

Kim, Jungho, Jungho Lee, Yangho Song, Heechan Han, and Jingul Joo. 2018. "Modeling the Runoff Reduction Effect of Low Impact Development Installations in an Industrial Area, South Korea." *Water* 10 (8): 967. https://doi.org/10.3390/w10080967.

Klein Tank, A. M. G., J. B. Wijngaard, G. P. Können, R. Böhm, G. Demarée, A. Gocheva, M. Mileta, et al. 2002. "Daily Dataset of 20th-Century Surface Air Temperature and Precipitation Series for the European Climate Assessment." *International Journal of Climatology* 22 (12): 1441–1453. https://doi.org/10.1002/joc.773.

Kottek, Markus, Jürgen Grieser, Christoph Beck, Bruno Rudolf, and Franz Rubel. 2006. "World Map of the Köppen-Geiger Climate Classification Updated." *Meteorologische Zeitschrift* 15 (3): 259–263. https://doi.org/10.1127/0941-2948/2006/0130.

Li, Ming-Han, and Michael E. Barrett. 2008. "Relationship Between Antecedent Dry Period and Highway Pollutant: Conceptual Models of Buildup and Removal Processes." *Water Environment Research* 80 (8): 740–747. https://doi.org/10.2175/106143008X296451.

Meteo France Public data portal. 2023. "Données Climatologiques de Base." Accessed July 25, 2023. https://publitheque.meteo.fr.

Miller, James D., and Michael Hutchins. 2017. "The Impacts of Urbanisation and Climate Change on Urban Flooding and Urban Water Quality: A Review of the Evidence Concerning the United Kingdom." *Journal of Hydrology: Regional Studies* 12 (August): 345–362. https://doi.org/10.1016/j.ejrh.2017.06.006.

Moftakhari, Hamed R., Amir AghaKouchak, Brett F. Sanders, Maura Allaire, and Richard A. Matthew. 2018. "What is Nuisance Flooding? Defining and Monitoring an Emerging Challenge." *Water Resources Research* 54 (7): 4218–4227. https://doi.org/10.1029/2018WR022828.

Murphy, Louise U., Thomas A. Cochrane, and Aisling O'Sullivan. 2015. "Build-Up and Wash-Off Dynamics of Atmospherically Derived Cu, Pb, Zn and TSS in Stormwater Runoff as a Function of Meteorological Characteristics." *Science of the Total Environment* 508 (March): 206–213. https://doi.org/10.1016/j.scitotenv.2014.11.094.

Nehls, Thomas, M. Menzel, and G. Wessolek. 2015. "Depression Storage Capacities of Different Ideal Pavements as Quantified by a Terrestrial Laser Scanning-Based Method." *Water Science & Technology* 71 (6): 862–869. https://doi.org/10.2166/wst.2015.025.

Ochoa-Rodriguez, Susana, Li-Pen Wang, Auguste Gires, Rui Daniel Pina, Ricardo Reinoso-Rondinel, Guendalina Bruni, Abdellah Ichiba, et al. 2015. "Impact of Spatial and Temporal Resolution of Rainfall Inputs on Urban Hydrodynamic Modelling Outputs: A Multi-Catchment Investigation." *Journal of Hydrology* 531 (December): 389–407. https://doi.org/10.1016/j.jhydrol.2015.05.035.

Paton, Eva, and Nasrin Haacke. 2021. "Merging Patterns and Processes of Diffuse Pollution in Urban Watersheds: A Connectivity Assessment." *WIREs Water* 8 (4): e1525. https://doi.org/10.1002/wat2.1525.

Qiu, Jiali, Zhenyao Shen, Guoyong Leng, and Guoyuan Wei. 2021. "Synergistic Effect of Drought and Rainfall Events of Different Patterns on Watershed Systems." *Scientific Reports* 11 (1): 18957. https://doi.org/10.1038/s41598-021-97574-z.

Rahimi, L., C. Deidda, and C. De Michele. 2021. "Origin and Variability of Statistical Dependencies Between Peak, Volume, and Duration of Rainfall-Driven Flood Events." *Scientific Reports* 11 (1): 5182. https://doi.org/10.1038/s41598-021-84664-1.

Raimbault, Georges, Hervé Andrieu, Emmanuel Berthier, Claude Joannis, and Michel Legret. 2002. "Infiltration Des Eaux Pluviales à Travers Les Surfaces Urbaines Des Revêtements Imperméables Aux Structures-Réservoir." *Bulletin Des Laboratoires Des Ponts et Chaussées* 5(238). https://trid.trb.org/View/951947.

Rivoire, Pauline, Olivia Martius, and Philippe Naveau. 2021. "A Comparison of Moderate and Extreme ERA-5 Daily Precipitation with Two Observational Data Sets." *Earth & Space Science* 8 (4): e2020EA001633. https://doi.org/10.1029/2020EA001633.

Rossman, Lewis, and Wayne C. Huber. 2016. *Storm Water Management Model Reference Manual Volume I – Hydrology*. Washington, DC, USA: USEPA.

Rossman, Lewis, and Simon Michelle. 2022. Storm Water Management Model User's Manual Version 5.2. Washington, DC, USA: USEPA.

Rubel, Franz, Katharina Brugger, Klaus Haslinger, and Ingeborg Auer. 2017. "The Climate of the European Alps: Shift of Very High Resolution Köppen-Geiger Climate Zones 1800–2100." *Meteorologische Zeitschrift* 26 (2): 115–125. https://doi.org/10.1127/metz/2016/0816.

Schär, Christoph, Nikolina Ban, Erich M. Fischer, Jan Rajczak, Jürg Schmidli, Christoph Frei, Filippo Giorgi, et al. 2016. "Percentile Indices for Assessing Changes in Heavy Precipitation Events." *Climatic Change* 137 (1–2): 201–216. https://doi.org/10.1007/s10584-016-1669-2.

Serra, C., A. Burgueño Xavier Lana, M. D. Martínez, and M. D. Martínez. 2016. "Partial Duration Series Distributions of the European Dry Spell Lengths for the Second Half of the Twentieth Century." *Theoretical and Applied Climatology* 123 (1–2): 63–81. https://doi.org/10.1007/s00704-014-1337-2.

Skougaard Kaspersen, P., N. Høegh Ravn, K. Arnbjerg-Nielsen, H. Madsen, and M. Drews. 2017. "Comparison of the Impacts of Urban Development and Climate Change on Exposing European Cities to Pluvial Flooding." *Hydrology and Earth System Sciences* 21 (8): 4131–4147. https://doi.org/10.5194/hess-21-4131-2017.

Soltaninia, Shahokh, Lobat Taghavi, Seyed Abbas Hosseini, Baharak Motamedvaziri, and Saeid Eslamian. 2023. "The Effects of Antecedent Dry Days and Land Use Types on Urban Runoff Quality in a Semi-Arid Region." *International Journal of Urban Sciences* 27 (2): 215–238. https://doi.org/10.1080/12265934.2022.2114928.

State Meteorological Agency AEMET. 2023. "Historical 10min Precipitation Data." Accessed July 25, 2023.

Vorobevskii, Ivan, Jeongha Park, Dongkyun Kim, Klemens Barfus, and Rico Kronenberg. 2024. "Simulating Sub-Hourly Rainfall Data for Current and Future Periods Using Two Statistical Disaggregation Models: Case Studies from Germany and South Korea." *Hydrology and Earth System Sciences* 28 (2): 391–416. https://doi.org/10.5194/hess-28-391-2024.

Wang, Zhenyu, Pei Hua, Heng Dai, Rui Li, Beidou Xi, Dongwei Gui, Jin Zhang, and Peter Krebs. 2020. "Influence of Surface Properties and Antecedent Environmental Conditions on Particulate-Associated Metals in Surface Runoff." *Environmental Science and Ecotechnology* 2 (April): 100017. https://doi.org/10.1016/j.ese.2020.100017.

Whitford, Anna C., Stephen Blenkinsop, David Pritchard, and Hayley J. Fowler. 2023. "A Gauge-Based Sub-Daily Extreme Rainfall Climatology for Western Europe." *Weather and Climate Extremes* 41 (September): 100585. https://doi.org/10.1016/j.wace.2023.100585.

World Meteorological Organisation. 2021. "Centennial Observing Stations, State of Recognition Report – 2021." https://public.wmo.int/en/our-mandate/what-we-do/observations/centennial-observing-stations.

Yang, Wenyu, Jin Zhang, Shenbin Mei, and Peter Krebs. 2021. "Impact of Antecedent Dry-Weather Period and Rainfall Magnitude on the Performance of Low Impact Development Practices in Urban Flooding and Non-Point Pollution Mitigation." *Journal of Cleaner Production* 320 (October): 128946. https://doi.org/10.1016/j.jclepro.2021.128946.

Yen, Ben C. 2001. "Hydraulics of Sewer Systems." *Stormwater Collection Systems Design Handbook*.

Zaherpour, Jamal, Simon N Gosling, Nick Mount, Hannes Müller Schmied, Ted I E Veldkamp, Rutger Dankers, Stephanie Eisner, et al. 2018. "Worldwide Evaluation of Mean and Extreme Runoff from Six Global-Scale Hydrological Models That Account for Human Impacts." *Environmental Research Letters* 13 (6): 065015. https://doi.org/10.1088/1748-9326/aac547.

APPENDICES

Appendix I: Impact of depression storages (ds) on runoff coefficient

Different depression storages (ds) of 1, 2, 5 and 10 mm were used in the SWMM model to estimate the corresponding runoff coefficients for the 10 European cities (Table A1).

Table A1. Runoff coefficients for the 10 European cities corresponding to depression storages of 1, 2, 5 and 10 mm.

	Runoff coefficient			
	ds =1 mm	ds = 2 mm	ds = 5 mm	ds =10 mm
Aarhus	0.77	0.7	0.61	0.46
Copenhagen	0.71	0.66	0.55	0.48
Hamburg	0.75	0.69	0.6	0.48
Berlin	0.73	0.65	0.51	0.40
Essen	0.79	0.73	0.63	0.54
Paris	0.76	0.69	0.58	0.42
Dunkirk	0.75	0.68	0.59	0.48
Bordeaux	0.78	0.72	0.62	0.53
Santiago de Compostela	0.88	0.84	0.8	0.75
Bilbao	0.85	0.80	0.74	0.64

Appendix II: SWMM model parameters for fully sealed and partially permeable scenarios

Table B1. SWMM parameters for fully sealed and partially permeable scenarios.

	Parameters	Value
General (for both scenarios)	Length of street section (m)	100
	Width (m)	10
	Street slope (%)	1
	Depression storage (mm)	2
	Manning's coefficient (asphalt road)	0.015
	Infiltration rate (asphalt road) (mm/hr)	0.036
Scenario 1: fully sealed street	Manning's coefficient (concrete side walk)	0.017
	Infiltration rate (concrete side walk) (mm/hr)	0.036
Scenario 2: partially permeable street	**Surface layer roughness**	0.023
	Pavement layer:	
	Thickness (mm), Impervious fraction	150, 0.9
	Permeability (mm/hr)	254
	Soil layer:	
	Thickness (mm)	250
	Conductivity (mm/h)	3.3
	Storage layer:	
	Thickness (mm)	200
	Filtration rate (mm/hr)	750

Parameters of asphalt road and concrete sidewalk are summarized from Rossman and Michelle (2022), Yen (2001). Parameters of block pavers are summarized from Rossman and Michelle (2022) and Chui, Liu, and Zhan (2016).